Current Biology 21, 1111–1117, July 12, 2011 ©2011 Elsevier Ltd All rights reserved DOI 10.1016/j.cub.2011.05.007

Report

# Retromer Controls Epithelial Cell Polarity by Trafficking the Apical Determinant Crumbs

Shirin Meher Pocha,[1] Thomas Wassmer,[2,3,*] Christian Niehage,[2] Bernard Hoflack,[2] and Elisabeth Knust[1,*]
[1]Max Planck Institute for Molecular Cell Biology and Genetics, Pfotenhauerstrasse 108, 01307 Dresden, Germany
[2]Biotechnologisches Zentrum der TU Dresden, Tatzberg 47/49, 01307 Dresden, Germany
[3]School of Life and Health Sciences, Aston University, Aston Triangle, Birmingham B4 7ET, UK

## Summary

**The evolutionarily conserved apical determinant Crumbs (Crb) is essential for maintaining apicobasal polarity and integrity of many epithelial tissues [1]. Crb levels are crucial for cell polarity and homeostasis, yet strikingly little is known about its trafficking or the mechanism of its apical localization. Using a newly established, liposome-based system described here, we determined Crb to be an interaction partner and cargo of the retromer complex. Retromer is essential for the retrograde transport of numerous transmembrane proteins from endosomes to the *trans*-Golgi network (TGN) and is conserved between plants, fungi, and animals [2]. We show that loss of retromer function results in a substantial reduction of Crb in *Drosophila* larvae, wing discs, and the follicle epithelium. Moreover, loss of retromer phenocopies loss of *crb* by preventing apical localization of key polarity molecules, such as atypical protein kinase C (aPKC) and Par6 in the follicular epithelium, an effect that can be rescued by overexpression of Crb. Additionally, loss of retromer results in multilayering of the follicular epithelium, indicating that epithelial integrity is severely compromised. Our data reveal a mechanism for Crb trafficking by retromer that is vital for maintaining Crb levels and localization. We also show a novel function for retromer in maintaining epithelial cell polarity.**

## Results

We aimed to identify factors that interact with the cytoplasmic domain of the type I transmembrane protein Crumbs (Crb) and are involved in its trafficking. We devised a strategy to present the Crb cytoplasmic tail on liposomes, a method uniquely suited to recruit and identify coats, because it mimics the native configuration of a receptor tail at the membrane/cytosol interface [3, 4].

### The Crb Intracellular Domain Interacts with Vps35

Proteoliposomes have been used successfully to identify coat complexes and their accessory proteins [3, 4]; however, these studies were restricted to short, chemically synthesized peptides, which severely limited the length of the cytoplasmic tail. To overcome this, we redesigned the recruitment assay enabling the use of tails expressed and purified from *E. coli*. We designed a bacterial expression plasmid containing an N-terminal tandem affinity tag followed by a tobacco etch virus (TEV) protease cleavage site and a single cysteine for the chemical coupling to liposomes, to which we fused the cytoplasmic tail of mouse Crb2 (amino acids R1246 to I1282) (Figures 1A–1C; see also Supplemental Experimental Procedures available online).

Because the levels of many transmembrane proteins are regulated by sorting decisions in the early (sorting) endosome, we incorporated phosphatidylinositol 3-phosphate, the predominant inositol phospholipid of early endosomes [5], into proteoliposomes to selectively enrich endosomal trafficking proteins. These proteoliposomes were used for recruiting cytosolic coat components and other interactors from brain extract [3, 6], followed by protein identification by tandem mass spectrometry (MS/MS). We chose *Crb2*, because it is the predominant *Crb* gene expressed in the vertebrate brain [7]. Importantly, the tails of all Crb proteins are highly conserved (Figure S1A), suggesting that their trafficking mechanisms may also be conserved. Mass spectroscopic analysis confirmed that large amounts of Crb2 (~600 $MS^2$ spectra) were coupled onto the liposomes. The most abundant protein isolated (as determined by $MS^2$ spectra) with an established role in the recognition and trafficking of transmembrane cargoes was the retromer subunit Vps35 (41 $MS^2$ spectra, 23.9% sequence coverage). In addition, we identified Vps26B (6 $MS^2$ spectra, 17.6% coverage). Western blotting confirmed the presence of Vps35 in our Crb2 recruitment reactions and showed it to be highly enriched relative to two independent controls (described in the Supplemental Experimental Procedures) (Figure 1D).

The mammalian retromer is composed of a cargo recognition subcomplex containing Vps35, Vps26, and Vps29 and a membrane interacting subcomplex consisting of SNX1/SNX2 and SNX5/SNX6 heterodimers [2]. Because both Vps35 and Vps26 are crucial for cargo recognition and binding, the recruitment data suggest that Crb2 is a retromer cargo.

To probe the hypothesis that Crb is a retromer cargo, we performed internalization assays by overexpressing FlaghCrb2 in HeLa cells and analyzing the uptake of anti-Flag antibodies, visualizing compartments through which Crb2 traffics. Previous studies using the classical retromer cargo, the cation-independent mannose-6-phosphate receptor (ciMPR), have shown that retromer subunits and cargo decorate tubules that emanate from endosomes and travel toward the *trans*-Golgi network (TGN) [8–10]. We observed colocalization of Crb2 with Vps35 on intracellular vesicles and tubules as well as an overlap with ciMPR- and galactosyltransferase (GalT) label (Figures S1B–S1F). These data suggest that in HeLa cells, Crb2 travels in retromer-decorated tubules and can traffic via the TGN. However, it should be noted that it does not accumulate there like other retromer cargoes (e.g., ciMPR). Instead, Crb2 appears to undergo rapid transport back to the plasma membrane. RNA interference (RNAi) suppression of Vps35 in HeLa cells displays enhanced localization of Crb2 in lysosomal structures positive for Lamp-I (Figures S1F–S1H), a phenotype described previously for other retromer cargoes [11]. These data are all in line with Crb being a potential retromer cargo.

*Correspondence: knust@mpi-cbg.de (E.K.), t.wassmer@aston.ac.uk (T.W.)

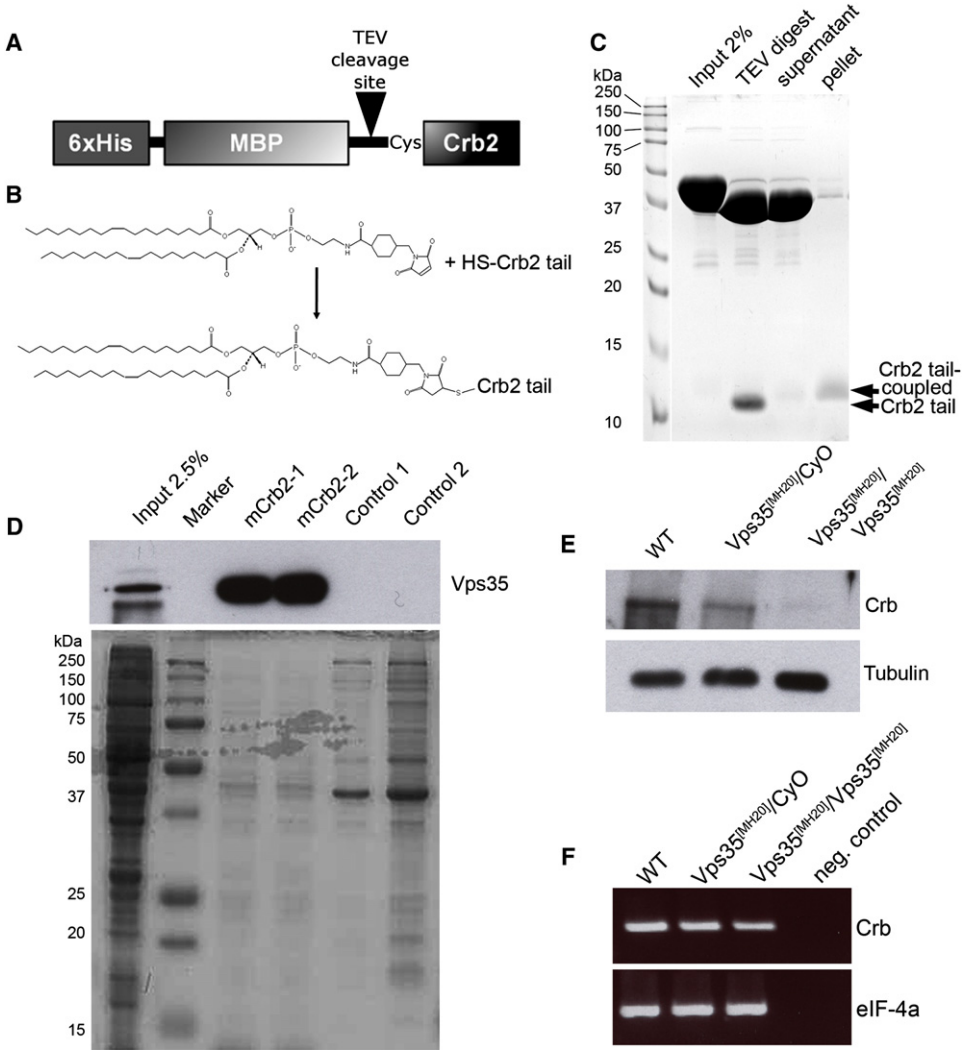


Figure 1. The Crb Intracellular Domain Recruits Vps35

(A) Scheme of the Crumbs (Crb) tail expression construct.

(B) Chemical coupling reaction of the cysteine sulfhydryl introduced into the Crb2 tail with the maleimide-activated lipid anchor, resulting in Crb tail coupling to liposomes.

(C) Coomassie-stained protein gel of the purified tandem-tagged Crb tail, cleavage of the tag, and coupling to liposomes that can be pelleted by centrifugation. The tandem tag was designed to not contain any cysteines and therefore is not coupled to liposomes. The Crb peptide displays modified gel migration behavior after coupling, presumably caused by the covalently attached lipid.

(D) Western blot of two independent Crb recruitment assays probed with anti-Vps35 antibody (top) showing a strong recruitment of Vps35 in Crb samples while being undetectable in two independent, negative controls (described in the Supplemental Experimental Procedures), despite relative underloading as shown by Coomassie staining of the recruitments (bottom).

(E) Western blots from third-instar wild-type (WT) and *Vps35*$^{[MH20]}$ hetero- and homozygote *Drosophila* larvae probed for Crb and tubulin as a loading control demonstrating a dose-dependent loss of Crb (longer blot exposure times confirm that some Crb protein is still present in the *Vps35*$^{[MH20]}$ homozygote lane; data not shown).

(F) PCR of Crb and eIF-4a using mRNA extracted from third-instar WT and *Vps35*$^{[MH20]}$ hetero- and homozygote *Drosophila* larvae, showing that Crb mRNA levels are largely unaffected by loss of Vps35, suggesting that the dramatic reduction of Crb protein in *Vps35* mutant tissue occurs posttranscriptionally. In the negative (neg.) control, cDNA was replaced with water.

## Loss of Retromer Function Leads to Loss of Crb

To study the functional interaction between Crb and retromer in *Drosophila*, we used a previously generated null allele of *Vps35*, *Vps35*$^{[MH20]}$ [12]. As a result of strong maternal contribution, animals homozygous for this allele reach the third larval instar [12], allowing us to analyze Crb in homozygous mutants. Because retromer is required for the retrieval of receptors from endosomes and thus the prevention of their lysosomal degradation [11, 13], we analyzed total Crb levels and found them to be reduced in *Vps35*$^{[MH20]}$ heterozygote third-instar larvae compared to stage-matched wild-type (WT) larvae and dramatically reduced in *Vps35*$^{[MH20]}$ homozygotes (Figure 1E). Analysis of the mRNA levels of Crb showed that loss of Vps35 has very little effect on *crb* transcripts (Figure 1F), suggesting that the dramatic reduction in Crb protein we see is due to posttranscriptional regulation of Crb by Vps35.

This led us to investigate Crb at a cellular level. For this, we chose two different epithelia, wing discs of third-instar larvae and the follicle epithelium. Clones of *Vps35*$^{[MH20]}$ mutant cells

in wing disc epithelia, labeled with GFP using the mosaic analysis with a repressible cell marker (MARCM) system [14], were induced by heat shock-Flp at early larval stages (confirmed in Figures S2A and S2B). Crb localizes to the subapical region of wing disc epithelial cells. In agreement with results from western blot analysis, Crb staining is decreased in *Vps35*$^{[MH20]}$ clones (Figure 2A). Quantification of the fluorescence intensity in the clone and in surrounding tissues revealed that there is an ~50% reduction in Crb signal within *Vps35*$^{[MH20]}$ clones (Figures 2B and 2C). The wing discs of *Vps35*$^{[MH20]}$ homozygous animals are small and show variable morphological defects, presumably as a result of defective Wingless secretion [15]. Analysis of Crb localization (by immunofluorescence) and protein levels (by western blotting) in *Vps35*$^{[MH20]}$ hetero- and homozygous wing discs corroborated the data that we obtained using *Vps35*$^{[MH20]}$ clones and larval lysate, respectively (Figures S2C–S2E).

The stability of the cargo-selective retromer subcomplex is dependent on the presence of all of its components [8, 16]. To show that the loss of Crb we see is due to loss of retromer function rather than just the loss of Vps35, we compared the effect of Vps26 and Vps35 knockdown in the posterior compartment of the wing disc using *engrailed-Gal4* [17] to drive *UAS-Vps26*$^{RNAi}$ and *UAS-Vps35*$^{RNAi}$. Hedgehog expression, which is unperturbed by loss of retromer [12], served to label the posterior compartment [18] (Figure 2D). Expression of either RNAi construct resulted in a clear reduction of Crb staining in the posterior compartment (~50% reduction in fluorescence; Figures 2D and 2E). Expression of *engrailed-Gal4* alone had no effect on Crb (Figures 2D and 2E). From these data, we conclude that the retromer cargo recognition subcomplex is required for the maintenance of Crb levels.

### Retromer Mutants Phenocopy *crb* Mutants in the Follicle Epithelium

To further analyze the relation between Crb and retromer, we turned to the follicular epithelium, which surrounds the germline cysts of the *Drosophila* ovary. Previous work has identified key roles for Crb in polarization of the follicular epithelium [19, 20]. Crb localizes to the entire apical membrane of the follicle epithelial cells, with very little detectable in the cytoplasm [19, 20] (Figure 3A). *Vps35*$^{[MH20]}$ clones show strong reduction in Crb staining (Figure 3A) and protein loss from the apical membrane. Interestingly, although Crb staining at the apical membrane is strongly reduced, it is not detected at increased levels within the cytoplasm, suggesting that Crb is not merely mislocalized but reduced at the protein level, as shown in larvae (Figure 1E). The cytoplasmic domain of Crb organizes an apical, membrane-associated protein complex by recruiting the scaffolding proteins Stardust (Sdt), *D*PATJ, and *D*Lin-7 [1]. Therefore, we assessed the apical localization of Sdt in the follicular epithelium and found that it is heavily reduced in *Vps35*$^{[MH20]}$ clones (Figure 3B). Probing whole larval lysates from third-instar WT and *Vps35*$^{[MH20]}$ hetero- and homozygotes for Sdt confirmed that at the protein level, like Crb (Figure 1E), Sdt shows a dose dependence on Vps35 (Figure S3A). Thus, retromer function in maintaining Crb levels and function is conserved between wing and follicle epithelia.

Interestingly, in some *Vps35*$^{[MH20]}$ clones, the strict monolayer structure of the epithelium is disrupted and the tissue appears multilayered (Figure 3B), an indication of polarity defects [21] and characteristic of loss of Crb at early stages of follicle development [20], whereas loss at later stages results only in the mislocalization of other polarity proteins, without affecting tissue integrity [19]. Multilayering was observed in 19% of *Vps35*$^{[MH20]}$ clones in follicles between stages 7 and 10 and did not appear to be dependent on clone size or position. Given that various links between Crb and Notch have been reported [22–25], we tested whether the multilayering phenotype observed in the follicle epithelium upon loss of *Vps35*$^{[MH20]}$ could be the result of defective Notch signaling. We analyzed the expression of Notch and Hindsight, a transcription factor downstream of Notch signaling that represses proliferation in the follicle epithelium [26], in *Vps35*$^{[MH20]}$ mutant clones. Both showed wild-type expression (Figures S3B and S3C), suggesting that Notch signaling is not affected by loss of retromer, similar to previous findings in the wing disc [12, 13, 27].

To test whether the loss of Crb in retromer mutants is due to missorting of Crb to the lysosome, we incubated follicles harboring *Vps35*$^{[MH20]}$ clones in leupeptin, a potent inhibitor of lysosomal proteases [8]. After a 3 hr incubation, we observed a dramatic accumulation of Crb in punctae within the cytoplasm of *Vps35*$^{[MH20]}$ cells (Figure 3C), a phenomenon that was not seen in WT tissue (Figure 3C) or in follicles containing *Vps35*$^{[MH20]}$ clones that were incubated in control medium lacking leupeptin (data not shown). Additionally, colocalization of these intracellular Crb punctae with LysoTracker was observed (Figure S3D). Together with the reduction of Crb protein levels and constant *crb* mRNA levels in *Vps35*$^{[MH20]}$ larvae and tissue, these data strongly suggest that retromer ablation leads to lysosomal degradation of Crb, as observed for other retromer cargoes [11, 13].

To test whether retromer functions after endocytosis of Crb, we blocked internalization of Crb from the plasma membrane by expression of a dominant-negative construct of *shibire* (dynamin) or by incubating follicles in dynasore, a dynamin inhibitor. In *Vps35*$^{[MH20]}$ clones, this resulted in the accumulation of Crb at the plasma membrane (Figures S4A and S4B), confirming that retromer is indeed transporting Crb after internalization from the plasma membrane.

Crb is required, together with atypical protein kinase C (aPKC), to restrict Bazooka/Par3 to the zonula adherens, an adhesion belt at the apex of epithelial cells, in the follicle epithelium, and in photoreceptor cells, thus excluding it from the apical membrane and specifying the border between apical and lateral domains [19, 28]. In previous studies, it was shown that the localization of aPKC and Par6 was dependent on Crb [19]. To test whether loss of retromer phenocopies the loss of Crb, we analyzed aPKC and Par6 localization in follicles containing *Vps35*$^{[MH20]}$ clones. Indeed, the level of both proteins is reduced at the apical surface in *Vps35*$^{[MH20]}$ clones (Figures 4A–4D). Interestingly, unlike Crb and the Crb complex member Sdt, Par6 and aPKC protein levels are not reduced in *Vps35*$^{[MH20]}$ mutant larvae (Figure S3A). Therefore, it is likely that the loss of Par6 and aPKC from the apical membrane of *Vps35*$^{[MH20]}$ clones in the follicle epithelium is due to loss of cell polarity in the absence of Crb rather than loss of the proteins themselves.

To test this, we overexpressed Crb in *Vps35*$^{[MH20]}$ clones. Because overexpression of Crb causes defects in epithelial cell polarity [29], we induced Crb overexpression using *GABFc204 Gal4*, a follicle epithelium-specific driver that starts expression late in follicle development (stage 8). Thereby, we were able to rescue the apical localization of Par6 (Figures 4E and 4F) and Sdt (Figure S4C). This rescue did not appear to be dependent on clone size or location. From these data, we conclude that the loss of polarity observed in retromer mutant clones is the direct result of loss of Crb.

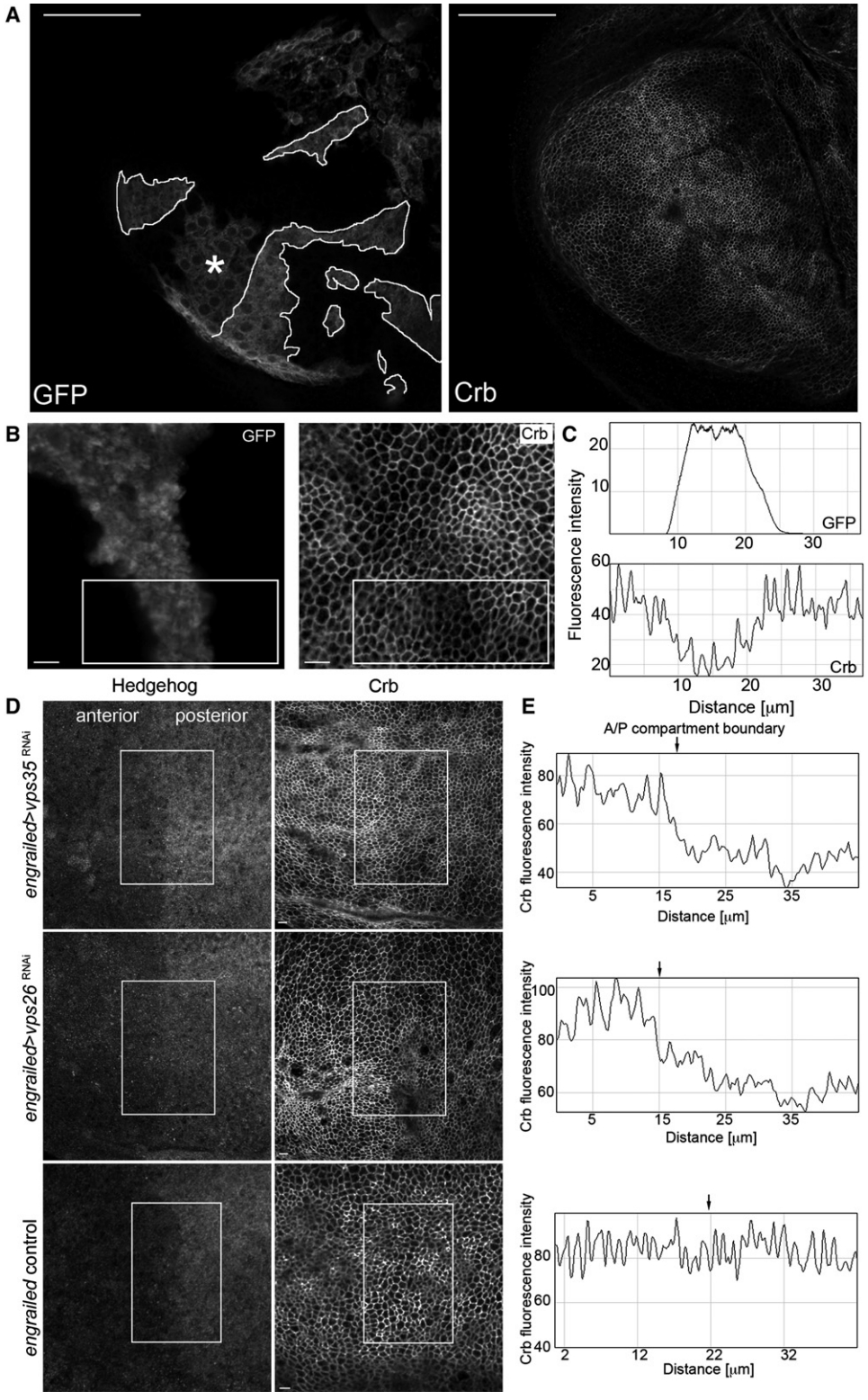


Figure 2. Crb Is Reduced in *Vps35*$^{[MH20]}$ Mutant Clones and upon RNAi-Mediated Knockdown of Vps26 and Vps35

(A) Third-instar wing disc pouch stained for GFP (marking *Vps35*$^{[MH20]}$ tissue) and Crb. White outlining depicts mutant clones only within the wing pouch to differentiate between those and clones within the peripodial membrane (the squamous cells above the pouch marked with an asterisk). Scale bar represents 50 μm.

(B) High-magnification image of third-instar wing discs stained for GFP (denotes *Vps35*$^{[MH20]}$ tissue) and Crb. Scale bar represents 5 μm.

(C) Profile plot of fluorescence intensity from the boxed region in (B).

(D) Third-instar wing discs of *engrailed-Gal4>Vps35RNAi* and *engrailed-Gal4>Vps26RNAi* animals stained for Hedgehog (marking the posterior compartment where *engrailed* is expressed) and Crb. *engrailed* control refers to *engrailed-Gal4* alone. White outlined sections are quantified in (E). Scale bars represent 5 μm.

(E) Quantification of the fluorescence intensity within the white outlined sections in (D), plotted along the A/P axis.

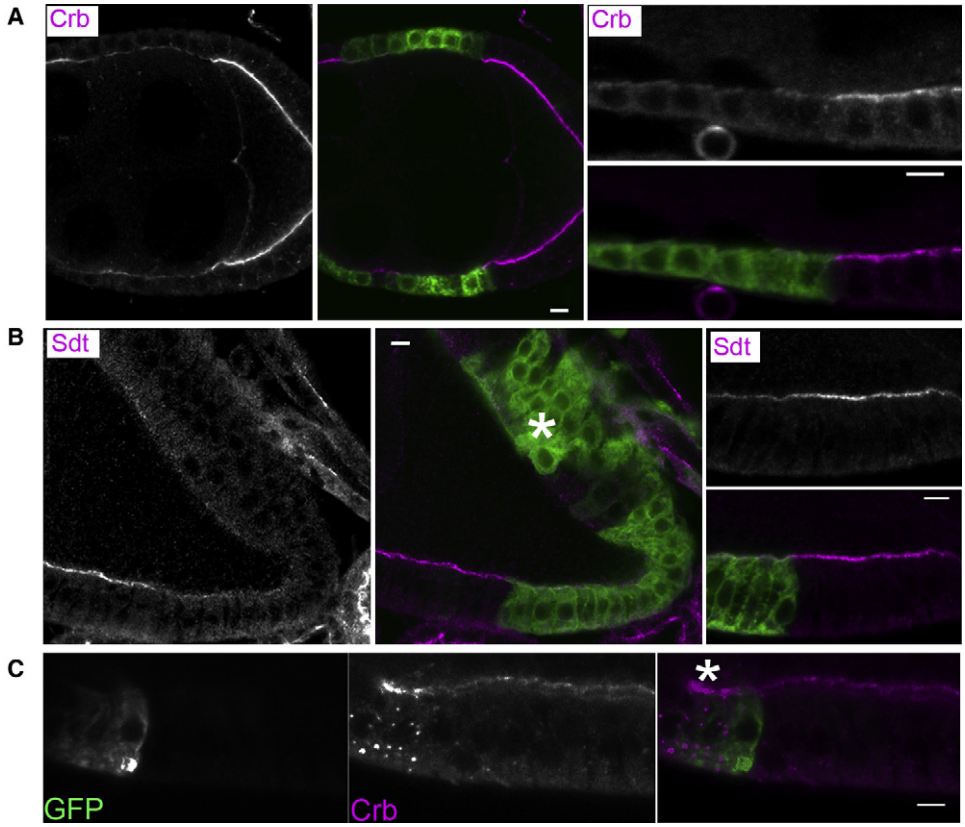


Figure 3. Loss of Vps35 in the Follicle Epithelium Leads to Loss of Crb from Apical Membranes and Results in Multilayering

(A and B) Follicles containing *Vps35*$^{[MH20]}$ clones (labeled with GFP) stained for Crb (stage 7) (A) and Sdt (stage 9) (B). Multilayering in the mutant clone is marked by an asterisk.

(C) Follicles containing *Vps35*$^{[MH20]}$ clones (labeled with GFP) incubated with the lysosomal protease inhibitor leupeptin for 3 hr and stained for Crb, showing accumulation of Crb in punctae within the cytoplasm of mutant cells when lysosomal function is compromised (stage 10). Increased Crb staining marked with an asterisk is likely due to increased Crb at the oocyte corners rather than at the apical pole of the follicular epithelium, often observed at this stage of follicle development. Scale bar represents 5 μm.

## Discussion

The identification of Crb as a retromer cargo confirms our hypothesis that one crucial step in the regulation of Crb occurs at the early (sorting) endosome and, importantly, fills a gap in the current understanding of Crb trafficking. Previous reports showed that transport of Crb to the plasma membrane is reliant on Rab11 [30], the exocyst [31, 32], and Cdc42 [33] in *Drosophila* embryonic epithelia. Internalization of Crb from the plasma membrane into endosomes is mediated by the syntaxin Avalanche and Rab5 [34]. Here we show that retromer is responsible for sorting Crb away from the degradative pathway and into a recycling one, thus allowing a high level of control over the amount of cellular Crb, previously shown to be vital for maintaining epithelial polarity and integrity, as demonstrated by numerous loss- and gain-of-function studies [29, 34–36]. Interestingly, retromer was previously shown to play a role in the apical delivery of the polymeric immunoglobulin receptor (pIgR) in Madin-Darby canine kidney cells [16]. However, as for Crb, it remains unclear whether this transport occurs via the TGN, via recycling endosomes, or through alternative pathways. The exact trafficking itinerary of Crb following recycling by retromer remains unclear and may depend upon the purpose of Crb recycling.

Which function of Crb is the prime target of retromer-driven retrieval? Is this a Crb level-sensing mechanism, in which retromer regulates the amount of protein at the plasma membrane, which is crucial for cell homeostasis? To date, all known functions of Crb require an intact Crb complex. By controlling the recycling of Crb and thereby its level at the plasma membrane, retromer could define the amount of Crb available for complex formation. Alternatively, it is tempting to speculate that Crb, much like Wntless (Wls), acts as a transport receptor and that apical delivery of its (yet to be identified) ligand or many ligands is the main purpose of its recycling to the TGN. These are fascinating hypotheses that will be the focus of future research.

### Supplemental Information

Supplemental Information includes four figures and Supplemental Experimental Procedures and can be found with this article online at doi:10.1016/j.cub.2011.05.007.

### Acknowledgments

We thank Maria Carvalho, Falko Riedel, Stephanie Spannl, Eurico Morais-de-Sá, and João Firmino for technical advice and the Aston Research Centre for Healthy Ageing microscopy facility at Aston University. We also thank Daniel St. Johnston, Suzanne Eaton, David Drechsel, Masaki

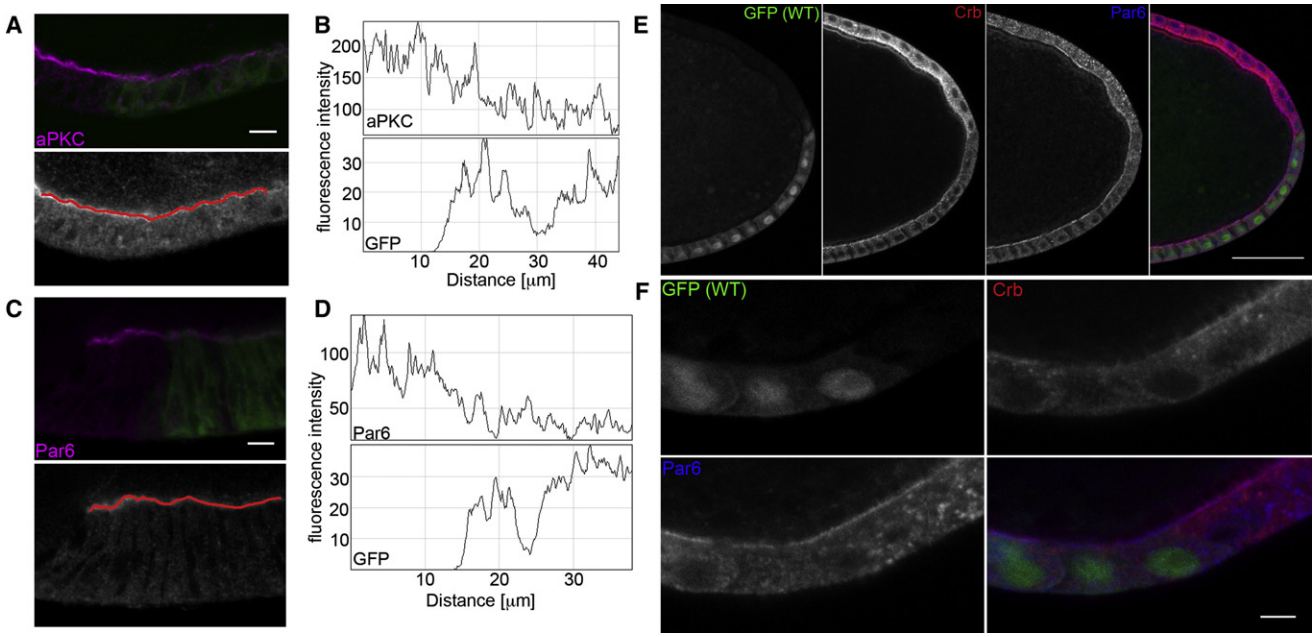


Figure 4. Loss of Vps35 in the Follicle Epithelium Phenocopies Loss of Crb by Reducing the Apical Localization of aPKC and Par6

(A and C) Follicles containing *Vps35[MH20]* clones (labeled with GFP) stained for aPKC (stage 7) (A) and Par6 (stage 10) (C). All scale bars represent 5 μm.
(B and D) Quantification of fluorescence intensity at the apical membrane (red line) in (A) and (C).
(E and F) Follicle containing *Vps35[MH20]* clones (note: identified by absence of GFP) and overexpressing Crb with *GABFc204 Gal4* in the mutant clone (stage 10), stained for Crb and Par6. Crb overexpression is sufficient to restore Par6 apical localization. Scale bar represents 50 μm in (E) and 5 μm in (F).

Nishimura, Jean Paul Vincent, Pen Rashbass, Andreas Wodarz, Thomas Widmann, and the Vienna Drosophila RNAi Center for reagents. We acknowledge Suzanne Eaton and Marino Zerial for constructive comments on the manuscript. This work was supported by the Max Planck Society (MPG) and a grant from the European Commission (HEALTH-F2-2008-200234) to E.K. and TransRegio 83, HO2584/1-2, HO2584/6-1, and HO2584/8-1 grants from the Deutsche Forschungsgemeinschaft to B.H.

Received: September 10, 2010
Revised: April 20, 2011
Accepted: May 5, 2011
Published online: June 23, 2011

## References

1. Bulgakova, N.A., and Knust, E. (2009). The Crumbs complex: From epithelial-cell polarity to retinal degeneration. J. Cell Sci. *122*, 2587–2596.
2. McGough, I.J., and Cullen, P.J. (2011). Recent advances in retromer biology. Traffic, in press. Published online May 23, 2011. 10.1111/j.1600-0854.2011.01201.x.
3. Baust, T., Czupalla, C., Krause, E., Bourel-Bonnet, L., and Hoflack, B. (2006). Proteomic analysis of adaptor protein 1A coats selectively assembled on liposomes. Proc. Natl. Acad. Sci. USA *103*, 3159–3164.
4. Crottet, P., Meyer, D.M., Rohrer, J., and Spiess, M. (2002). ARF1.GTP, tyrosine-based signals, and phosphatidylinositol 4,5-bisphosphate constitute a minimal machinery to recruit the AP-1 clathrin adaptor to membranes. Mol. Biol. Cell *13*, 3672–3682.
5. Di Paolo, G., and De Camilli, P. (2006). Phosphoinositides in cell regulation and membrane dynamics. Nature *443*, 651–657.
6. Baust, T., Anitei, M., Czupalla, C., Parshyna, I., Bourel, L., Thiele, C., Krause, E., and Hoflack, B. (2008). Protein networks supporting AP-3 function in targeting lysosomal membrane proteins. Mol. Biol. Cell *19*, 1942–1951.
7. van den Hurk, J.A., Rashbass, P., Roepman, R., Davis, J., Voesenek, K.E., Arends, M.L., Zonneveld, M.N., van Roekel, M.H., Cameron, K., Rohrschneider, K., et al. (2005). Characterization of the Crumbs homolog 2 (CRB2) gene and analysis of its role in retinitis pigmentosa and Leber congenital amaurosis. Mol. Vis. *11*, 263–273.
8. Arighi, C.N., Hartnell, L.M., Aguilar, R.C., Haft, C.R., and Bonifacino, J.S. (2004). Role of the mammalian retromer in sorting of the cation-independent mannose 6-phosphate receptor. J. Cell Biol. *165*, 123–133.
9. Carlton, J., Bujny, M., Peter, B.J., Oorschot, V.M., Rutherford, A., Mellor, H., Klumperman, J., McMahon, H.T., and Cullen, P.J. (2004). Sorting nexin-1 mediates tubular endosome-to-TGN transport through coincidence sensing of high- curvature membranes and 3-phosphoinositides. Curr. Biol. *14*, 1791–1800.
10. Wassmer, T., Attar, N., Harterink, M., van Weering, J.R., Traer, C.J., Oakley, J., Goud, B., Stephens, D.J., Verkade, P., Korswagen, H.C., and Cullen, P.J. (2009). The retromer coat complex coordinates endosomal sorting and dynein-mediated transport, with carrier recognition by the trans-Golgi network. Dev. Cell *17*, 110–122.
11. Seaman, M.N. (2004). Cargo-selective endosomal sorting for retrieval to the Golgi requires retromer. J. Cell Biol. *165*, 111–122.
12. Franch-Marro, X., Wendler, F., Guidato, S., Griffith, J., Baena-Lopez, A., Itasaki, N., Maurice, M.M., and Vincent, J.P. (2008). Wingless secretion requires endosome-to-Golgi retrieval of Wntless/Evi/Sprinter by the retromer complex. Nat. Cell Biol. *10*, 170–177.
13. Port, F., Kuster, M., Herr, P., Furger, E., Bänziger, C., Hausmann, G., and Basler, K. (2008). Wingless secretion promotes and requires retromer-dependent cycling of Wntless. Nat. Cell Biol. *10*, 178–185.
14. Lee, T., and Luo, L. (2001). Mosaic analysis with a repressible cell marker (MARCM) for Drosophila neural development. Trends Neurosci. *24*, 251–254.
15. Eaton, S. (2008). Retromer retrieves wntless. Dev. Cell *14*, 4–6.
16. Vergés, M., Luton, F., Gruber, C., Tiemann, F., Reinders, L.G., Huang, L., Burlingame, A.L., Haft, C.R., and Mostov, K.E. (2004). The mammalian retromer regulates transcytosis of the polymeric immunoglobulin receptor. Nat. Cell Biol. *6*, 763–769.
17. Eugster, C., Panáková, D., Mahmoud, A., and Eaton, S. (2007). Lipoprotein-heparan sulfate interactions in the Hh pathway. Dev. Cell *13*, 57–71.
18. Ingham, P.W., and McMahon, A.P. (2001). Hedgehog signaling in animal development: Paradigms and principles. Genes Dev. *15*, 3059–3087.
19. Morais-de-Sá, E., Mirouse, V., and St Johnston, D. (2010). aPKC phosphorylation of Bazooka defines the apical/lateral border in Drosophila epithelial cells. Cell *141*, 509–523.

20. Tanentzapf, G., Smith, C., McGlade, J., and Tepass, U. (2000). Apical, lateral, and basal polarization cues contribute to the development of the follicular epithelium during Drosophila oogenesis. J. Cell Biol. *151*, 891–904.
21. St Johnston, D., and Ahringer, J. (2010). Cell polarity in eggs and epithelia: Parallels and diversity. Cell *141*, 757–774.
22. Herranz, H., Stamataki, E., Feiguin, F., and Milán, M. (2006). Self-refinement of Notch activity through the transmembrane protein Crumbs: Modulation of gamma-secretase activity. EMBO Rep. *7*, 297–302.
23. Mitsuishi, Y., Hasegawa, H., Matsuo, A., Araki, W., Suzuki, T., Tagami, S., Okochi, M., Takeda, M., Roepman, R., and Nishimura, M. (2010). Human CRB2 inhibits gamma-secretase cleavage of amyloid precursor protein by binding to the presenilin complex. J. Biol. Chem. *285*, 14920–14931.
24. Pardossi-Piquard, R., Chen, F., Silva-Gagliardi, N.F., Szego, M., McInnes, R., McGlade, C.J., St George-Hyslop, P., and Fraser, P.E. (2007). Overexpression of human CRB1 or related isoforms, CRB2 and CRB3, does not regulate the human presenilin complex in culture cells. Biochemistry *46*, 13704–13710.
25. Richardson, E.C., and Pichaud, F. (2010). Crumbs is required to achieve proper organ size control during Drosophila head development. Development *137*, 641–650.
26. Sun, J., and Deng, W.-M. (2007). Hindsight mediates the role of notch in suppressing hedgehog signaling and cell proliferation. Dev. Cell *12*, 431–442.
27. Belenkaya, T.Y., Wu, Y., Tang, X., Zhou, B., Cheng, L., Sharma, Y.V., Yan, D., Selva, E.M., and Lin, X. (2008). The retromer complex influences Wnt secretion by recycling wntless from endosomes to the trans-Golgi network. Dev. Cell *14*, 120–131.
28. Walther, R.F., and Pichaud, F. (2010). Crumbs/DaPKC-dependent apical exclusion of Bazooka promotes photoreceptor polarity remodeling. Curr. Biol. *20*, 1065–1074.
29. Wodarz, A., Hinz, U., Engelbert, M., and Knust, E. (1995). Expression of crumbs confers apical character on plasma membrane domains of ectodermal epithelia of Drosophila. Cell *82*, 67–76.
30. Roeth, J.F., Sawyer, J.K., Wilner, D.A., and Peifer, M. (2009). Rab11 helps maintain apical crumbs and adherens junctions in the Drosophila embryonic ectoderm. PLoS ONE *4*, e7634.
31. Blankenship, J.T., Fuller, M.T., and Zallen, J.A. (2007). The Drosophila homolog of the Exo84 exocyst subunit promotes apical epithelial identity. J. Cell Sci. *120*, 3099–3110.
32. Campbell, K., Knust, E., and Skaer, H. (2009). Crumbs stabilises epithelial polarity during tissue remodelling. J. Cell Sci. *122*, 2604–2612.
33. Harris, K.P., and Tepass, U. (2008). Cdc42 and Par proteins stabilize dynamic adherens junctions in the Drosophila neuroectoderm through regulation of apical endocytosis. J. Cell Biol. *183*, 1129–1143.
34. Lu, H., and Bilder, D. (2005). Endocytic control of epithelial polarity and proliferation in Drosophila. Nat. Cell Biol. *7*, 1232–1239.
35. Pellikka, M., Tanentzapf, G., Pinto, M., Smith, C., McGlade, C.J., Ready, D.F., and Tepass, U. (2002). Crumbs, the Drosophila homologue of human CRB1/RP12, is essential for photoreceptor morphogenesis. Nature *416*, 143–149.
36. Richard, M., Muschalik, N., Grawe, F., Ozüyaman, S., and Knust, E. (2009). A role for the extracellular domain of Crumbs in morphogenesis of Drosophila photoreceptor cells. Eur. J. Cell Biol. *88*, 765–777.

**Current Biology, Volume *21***

# Supplemental Information

# Retromer Controls Epithelial Cell Polarity by Trafficking the Apical Determinant Crumbs

**Shirin Meher Pocha, Thomas Wassmer, Christian Niehage, Bernard Hoflack, and Elisabeth Knust**

## Supplemental Inventory

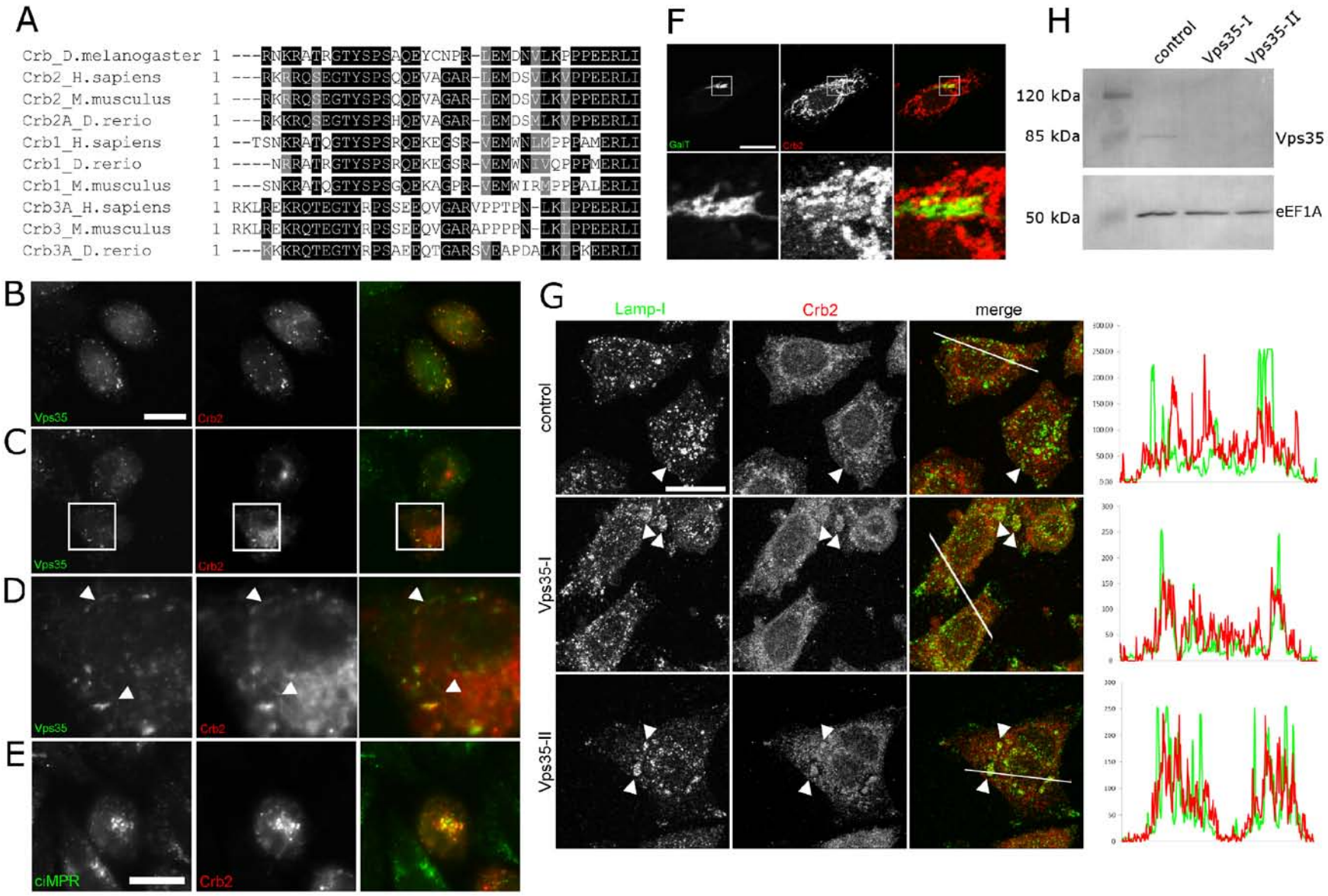
A
Crb_D.melanogaster 1 ---RNKRATRGTYSPSAQEYCNPR-LEMDNVLKPPPEERLI
Crb2_H.sapiens 1 ---RKHRQSEGTYSPSQQEVAGAR-LEMDSVLKVPPEERLI
Crb2_M.musculus 1 ---RKHRQSEGTYSPSQQEVAGAR-LEMDSVLKVPPEERLI
Crb2A_D.rerio 1 ---RKKRQSEGTYSPSHQEVAGAR-LEMDSMLKVPPEERLI
Crb1_H.sapiens 1 --TSNKRATQGTYSPSRQEKEGSR-VEMWNLKPPEAMERLI
Crb1_D.rerio 1 -----NRRATRGTYSPSRQEKEGSR-VEMWNIVQPPPMERLI
Crb1_M.musculus 1 ---SNKRATQGTYSPSGQEKAGPR-VEMWIRVPPEALERLI
Crb3A_H.sapiens 1 RKLREKRQTEGTYRPSSEEQVGARVPPTPN-LKLPPEERLI
Crb3_M.musculus 1 RKLREKRQTEGTYRPSSEEQVGARAPPPPN-LKLPPEERLI
Crb3A_D.rerio 1 ---KKKRQTEGTYRPSAEEQTGARSVEAPDALKLPKEERLI
F
GalT
Crb2
H
control
Vps35-I
Vps35-II
120 kDa
85 kDa
Vps35
50 kDa
eEF1A
B
Vps35
Crb2
C
Vps35
Crb2
D
Vps35
Crb2
E
ciMPR
Crb2
G
Lamp-I
Crb2
merge
control
Vps35-I
Vps35-II

**Figure S1, Related to Figure 1.**

(A) The cytoplasmic domains of Crb proteins from *Drosophila*, zebrafish, mouse and humans were aligned using the ClustalW algorithm. Note the high degree of sequence identity between drosophila Crb and mouse or human Crb2 (73% identity). Accession numbers utilised are: Crb_*D.melanogaster*: NP_524480; Crb1_H.sapiens: NP_957705; Crb2_H.sapiens: NP_775960; Crb3A_H.sapiens: NP_631900; Crb1_M.musculus: NP_573502; Crb2_M.musculus: NP_001157038; Crb3_M.musculus: NP_808306; Crb1_D.rerio: NP_001038408; Crb2a_D.rerio: NP_001038764; Crb3a_D.rerio: NP_001038787

(B–D) Flag-Crb2 transfected HeLa cells were incubated with Flag antibody to label compartments through which Crb2 traffics and co-stained for Vps35. Note the numerous vesicular structures in which Crb2 and Vps35 co-localize indicating that Crb2 traffics through retromer positive compartments.

(D) In this enlargement from (C) arrowheads indicate two Vps35 positive tubules that are co-stained for Crb2, suggesting that Crb2 traffics using retromer positive carriers described in [1, 2]. Scale bar 20 μm.

(E) Flag-Crb2 transfected HeLa cells were incubated with Flag antibody to label compartments through which Crb2 traffics and co-stained for the cation-independent mannose-6-phosphate receptor (ciMPR), which localizes at steady state to the trans-Golgi (TGN) network [3]. Co-localization with the Crb2 label indicates that Crb2 is sorted intracellularly via the TGN as observed for other retromer cargoes. Scale bar 20 μm.

(F) HeLa cells were cotransfected with Flag-Crb2 and YFP-Galactosyltransferase (GalT), an established TGN marker. Flag antibody uptake revealed colocalization in the TGN area, suggesting that Crb2 can traffic through the TGN. However, only little of the cellular Crb2 is concentrated in the TGN which is consistent with rapid exit of Crb from the TGN followed by trafficking to the plasma membrane.

(G) RNAi mediated suppression of Vps35 using two different siRNAs results in enhanced localization of Flag-Crb2 in lysosomes in HeLa cells. Flag-Crb2 was allowed to accumulate for 4 h in lysosomes in the presence of lysosomal inhibitors in the medium to limit potential degradation of Flag-Crb2. Arrowheads indicate lysosomal structures that display Crb2 labeling. Note that while in control cells little Crb2 can be detected in lysosomes there is considerable overlap between LAMP-I and Crb staining in Vps35 suppressed cells, as illustrated by the line scans for LAMP-I (green) and Crb2 (red).

(H) Western blotting for Vps35 demonstrates high knock-down efficiency relative to the loading control elongation factor 1A (eEF1A).

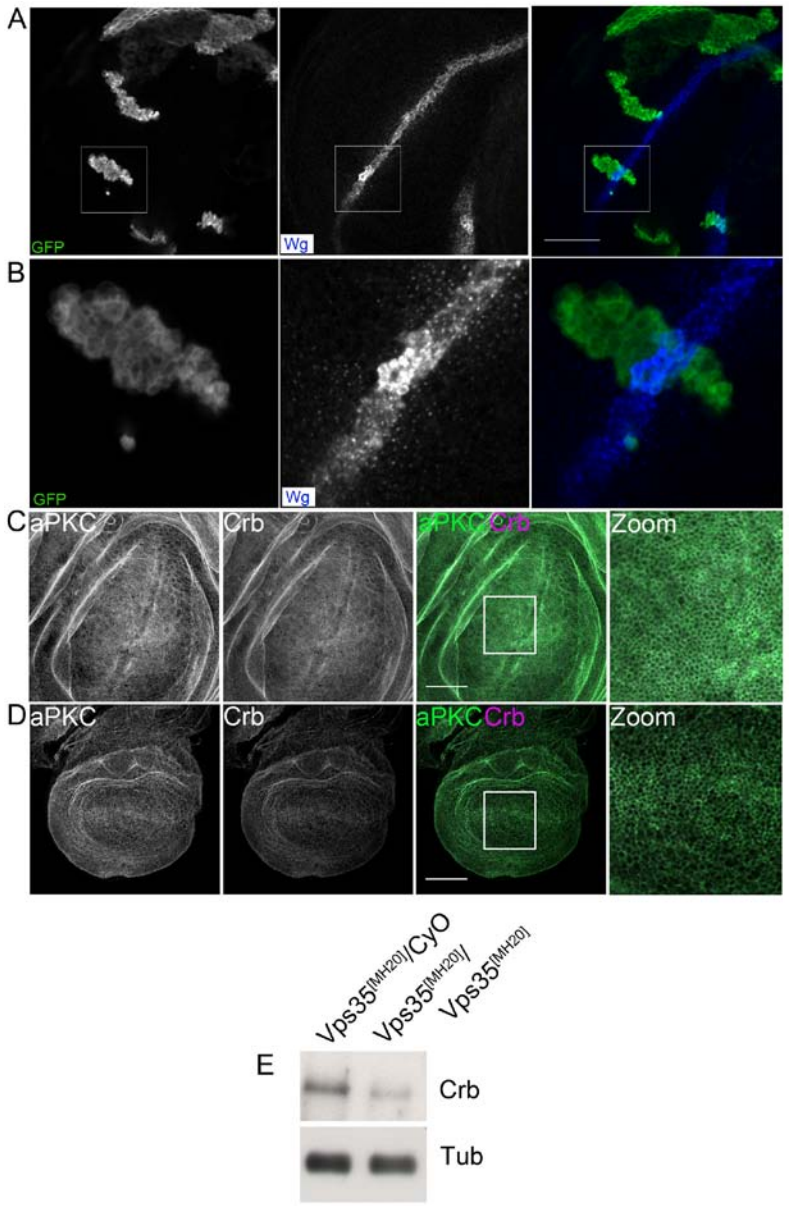


**Figure S2, Related to Figure 2.**

(A) 3rd instar wing discs stained for GFP (denotes *Vps35*$^{[MH20]}$ tissue) and Wg. Scale bar 50 μm.
(B) Zoom in on boxed region of (A) showing accumulation of Wg in Wg-expressing cells in the *Vps35*$^{[MH20]}$ tissue, and a reduction in the amount of secreted Wg seen in either side of the *Vps35*$^{[MH20]}$ clone.
(C and D) Wing discs from heterozygous (C) and homozygous (D) *Vps35*$^{[MH20]}$ stage-matched wandering 3rd instar larvae, respectively, stained for Crb and aPKC. Zoom panels show Crb and aPKC staining retains a honeycomb pattern despite reduced overall staining levels when comparing heterozygous and homozygous tissue. Scale bar 50 μm.
(E) Western blots from wing discs of heterozygous and homozygous *Vps35*$^{[MH20]}$ stage-matched wandering 3rd instar larvae probed for Crb and tubulin as a loading control. The reduction in Crb levels reflects results obtained with whole larval lysates.

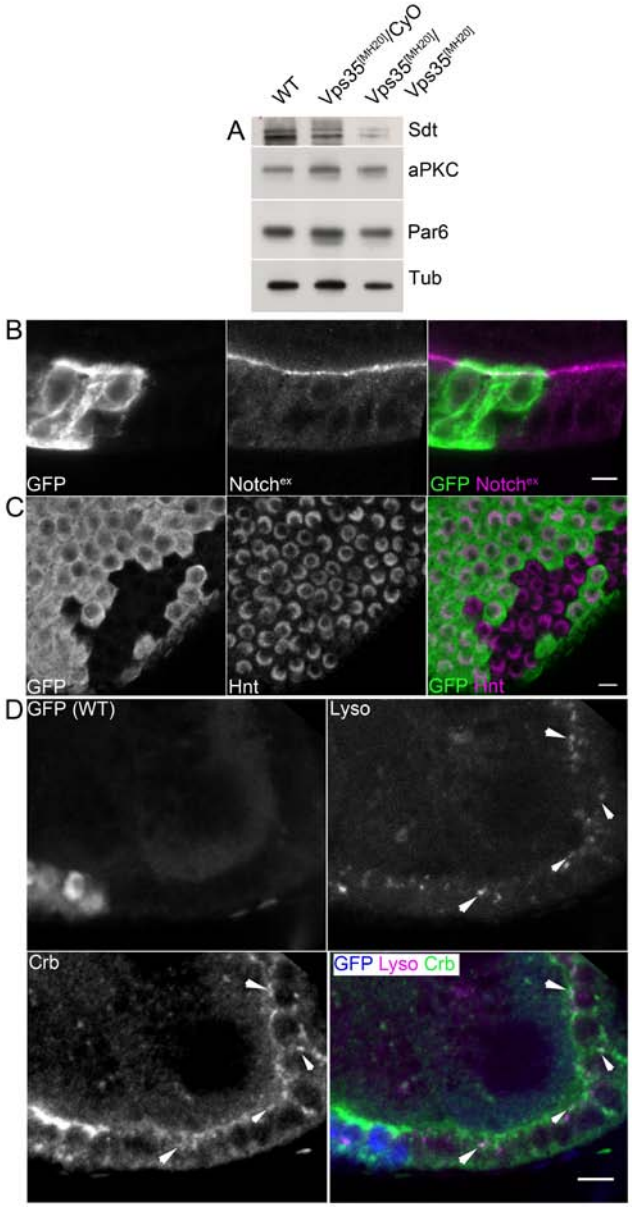


**Figure S3, Related to Figure 3.**

(A) Western blots from 3rd instar WT, *Vps35*$^{[MH20]}$ hetero- and homozygote *Drosophila* larvae probed for Stardust (Sdt), Par6, aPKC and tubulin as a loading control, showing that while Crb complex member Sdt is, like Crb, also reduced at a protein level, Par6 and aPKC are not affected by loss of Vps35.
(B and C) Follicles containing *Vps35*$^{[MH20]}$ clones (labeled with GFP) stained for Notch extracellular domain (B, stage 10) and Hindsight (Hnt, C, stage 9), both of which appear unaffected by loss of Vps35. Scale bar 5 μm.
(D) Follicles containing *Vps35*$^{[MH20]}$ clones (note: marked by absence of GFP) incubated with leupeptin for 3 hrs and Lysotracker (Lyso) for the last 1 hr then stained for Crb. Colocalisation of intracellular Crb punctae with Lysotracker is marked with arrowheads. Scale bar 5 μm.

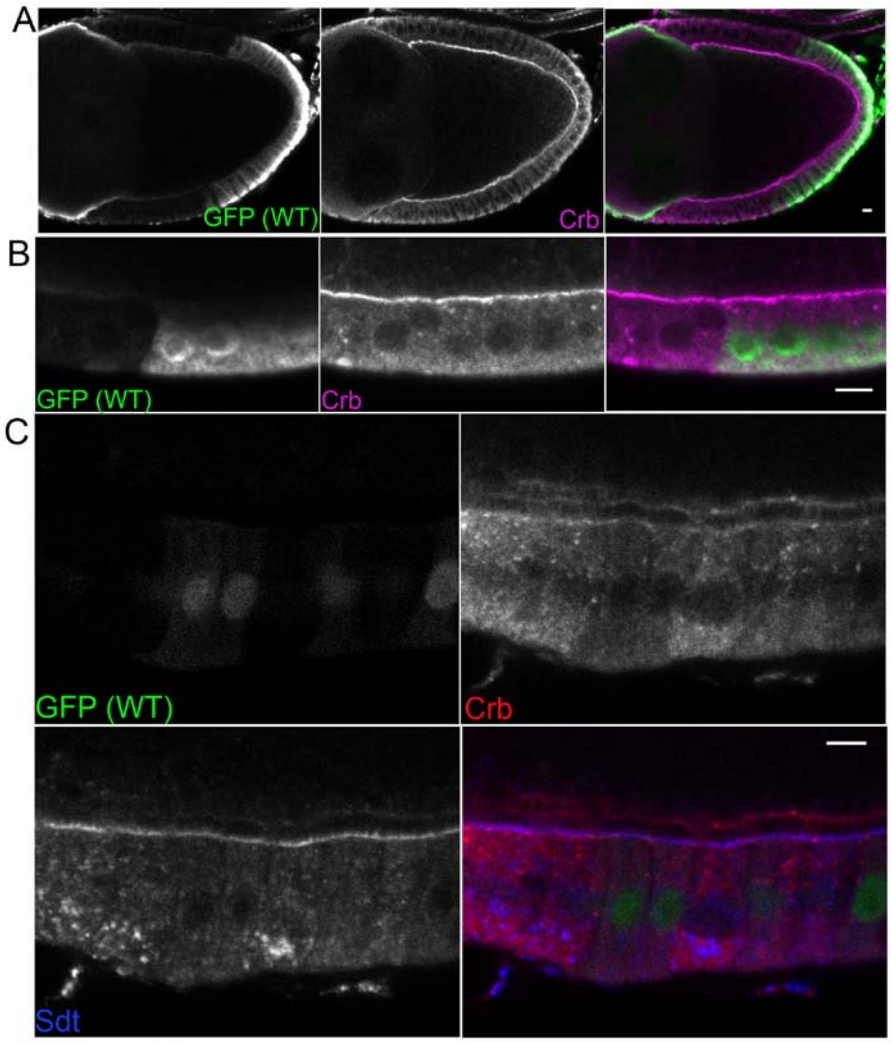


**Figure S4, Related to Figure 4.**

(A) Follicles containing *Vps35*$^{[MH20]}$ clones (note: marked by absence of GFP) and expressing dominant negative Shibire (ShiK44A) with *GABFc204 Gal4* (Stage 10), stained for Crb and GFP. Inhibition of *shibire* (dynamin) activity prevents internalization of Crb from the plasma membrane and therefore negates the loss of Crb staining seen in control *Vps35* mutant clones (not shown; compare with Fig. 3A), confirming that retromer acts after endocytic events at the plasma membrane. Scale bar 5 μm.
(B) Follicles containing *Vps35*$^{[MH20]}$ clones (note: marked by absence of GFP) incubated with 60 μM Dynasore for 1 hr (Stage 9), stained for Crb and GFP. Inhibition of *shibire* (dynamin) activity prevents internalization of Crb from the plasma membrane and therefore negates the loss of Crb staining seen in control Vps35 mutant clones (not shown; compare with Fig. 3A), confirming that retromer acts after endocytic events at the plasma membrane. Scale bar 5 μm.
(C) Follicles containing *Vps35*$^{[MH20]}$ clones (note: marked by absence of GFP) and overexpressing Crb with *GABFc204 Gal4* in the mutant clone (late stage 9), stained for Crb and Sdt. Crb overexpression is sufficient to restore Sdt apical localization. Note that some Sdt also localises to intracellular puncta that interestingly do not co-stain for Crb. Scale bar 5 μm.

## Supplemental Experimental Procedures

### Construction of the Expression Plasmid

We cloned the ORF fragment encoding K27 to K396 of the E. coli malE protein together with a TEV protease cleavage site (ENLYFQGS) using the NheI and BamHI restriction sites of the pET28 bacterial expression plasmid (Novagen) with standard PCR and cloning techniques (construct name: pET28-MBP-TEV). The mouse Crb2 tail (R1246 to I1282; Accession. No.: NM_001163566.1) was PCR amplified from a cDNA kindly provided by P. Rashbass and cloned into pET28-MBP-TEV using the BamHI and XhoI restriction sites, thereby introducing an additional cystein for coupling followed by a glycine for flexibility of the Crb2 tail.

### Protein Expression, Purification, and Coupling

Recombinant protein expression using the BL21DE3 expression strain (Novagen) and purification by metal affinity chromatography was performed using IMAC affinity resin (GE Healthcare) according to the manufacturer's instructions. Under standard expression conditions (100 µM IPTG, 37°C, 3 h) followed by affinity chromatography this construct yielded typically more than 25 mg of soluble, highly pure protein. Purified protein was dialysed into 20 mM Hepes KOH pH 7.2, 125 mM K-Acetate, 1 mM EDTA. For TEV-digest, ~300 µg of His-MBP-tagged protein was incubated at room temperature overnight with 2 mM Tris (2-carboxyethyl) phosphine (Pierce) and 2.5 µg recombinant TEV protease kindly provided by the protein purification facility of the Max Planck Institute for Molecular Cell Biology and Genetics, Dresden.

### Proteoliposome Preparation

Liposomes were prepared similar to [4]. Briefly, a mixture of phosphatidylcholine/ phosphatidylethanolamine/ phosphatidylserine/ cholesterol/ maleimide anchor (18:1 PE MCC, catalogue number 780201P, Avanti Polar Lipids) and phosphatidylinositole-3-phosphate (40:30:10:10:10:1 molar ratio) in chloroform/methanol were mixed and dried. Lipids were resuspended in Recruitment Buffer (RB) and liposomes were formed by repeated freeze-thaw cycles. Liposomes were then incubated for 1 hour at room temperature with either the TEV-released Crb2 tail, or as controls, either a non-related cysteine containing peptide or 1 mM cysteine. The liposomes were pelleted by centrifugation at 25,000 g for 15 min at room temperature, the supernatant discarded and the pellet washed once with RB to eliminate not incorporated peptide. Reactive maleimide groups were quenched with 5 mM 2-Mercaptoethanol for 30 min at RT. Recruitment reactions were performed as established in [4, 5].

### Sample Preparation for MS

Following recruitment the pellet was dissolved in 40µL 2x Laemmli sample buffer and 20µL were loaded onto a Tris-glycine PAGE gel. Following electrophoresis the gel was stained with Coomassie G-250. The whole lane was manually cut into 18 slices and embedded proteins were reduced with dithiothreitol (DTT), alkylated with iodoacetamide, digested over night with trypsin in a 1:50 ratio and subjected to LC-MS analysis as described previously [6].

### Mass Spectrometric Analysis

Peptides were separated on an EASY-nLC HPLC system (Proxeon, Odense, Denmark) equipped with a fused silica microcapillary C18 column (Proxeon, length 10 cm; inner diameter 75 µm; particle size 3 µm, 100 Å pore size). The gradient used was: A, 0.1% formic acid; B, acetonitrile, 0.1% formic acid with a final concentration of 80% B.

Mass spectrometric measurement was accomplished on a LTQ Orbitrap XL mass spectrometer (Thermo Fisher Scientific). The Xcalibur raw-files of all 18 gel slices corresponding to one sample were merged to one analysis using the Proteome Discoverer 1.1 software (Thermo

Fisher Scientific) and Scaffold 3.0 (Proteome Software Inc., Portland, OR, USA). The algorithms applied for the interpretation of tandem mass spectra were Mascot (without Identity Score) (Matrix Science, London, UK; version 1.1.0.263), Sequest (Thermo Fisher Scientific; version 1.1.0.263) and X! Tandem (The GPM, thegpm.org; version 2007.01.01.1) using the SwissProt database (SwissProt_56.9.fasta) for interpretation of spectra with the following settings: the taxonomy was set to mammalian for Mascot, a restricted database with pig, human mouse and rat entries only was used for Sequest. X!Tandem used only proteins identified by the two other algorithms. Trypsin was set as the enzyme allowing up to two missed cleavages. Precursor mass tolerance was set to 10 ppm, fragment mass tolerance to 0.8 Da. As a static modification carbamidomethylation (of cysteine) was chosen and as dynamic modifications deamidation (of asparagine and glutamine) and oxidation (of methionine). The Spectral Count method [7] was used for the detection of abundance changes of proteins in samples vs. control. Briefly, spectra leading to a high confident peptide identification and belonging to a certain protein on the receptor tail containing proteoliposomes where counted and compared to the counts for the same protein on liposomes without a coupled receptor tail.

**Genetics**

The *Vps35* null allele *Vps35*$^{[MH20]}$ was generated and characterized previously [8] and was a kind gift from J.P. Vincent. RNAi lines were obtained from the Vienna *Drosophila* RNAi Centre (http://www.vdrc.at), *UAS-Vps26*$^{RNAi}$ (18396) and *UAS-Vps35*$^{RNAi}$ (18396). These were driven exclusively in posterior compartments using *engrailed*$^{105}$*-Gal4* obtained from S. Eaton [9]. All flies were raised at 25ºC. MARCM clones were generated by crossing virgin *yw-hsFLP,UAS-GFP; tubP-Gal80 FRT42D; tubPGal4/TM6B* flies (T. Widmann [10]) to *FRT42D-Vps35*$^{[MH20]}$ */CyO* males. For rescue experiments, *UAS-Crb-Full length* (line Crb$^{wt-2e}$ previously described in [11]) was recombined with *FRT42D-Vps35*$^{[MH20]}$ and driven with *GABFc204-Gal4* (E. Morais-de-Sá). *UAS-ShiK44A* [12] was obtained from Bloomington Stock Centre. For wing disc or follicle clones, 37ºC heat shock was performed for 1.5 h on 1$^{st}$ instar larvae or 2 h on 3$^{rd}$ instar larvae, respectively.

**Antibodies**

The following antibodies were used in this study at the given dilutions for Western blotting (WB) or immunofluorescence (IF): Goat anti-Vps35 (BD-Biosciences), 1:500 (WB). Rabbit anti-Vps35 (Millipore) 1:200 (IF), 1:1000 (WB). Mouse anti-eEF1A (Millipore), 1:1000 (WB). Rat anti-Crb 2.8 [13], 1:1000 (WB and IF). Rat anti-alpha-Tubulin (Serotec), 1:5000 (WB). Mouse anti-Hedgehog and anti-Wingless, 1:500 (IF) were both gifts from S. Eaton. Rabbit anti-GFP (Invitrogen), 1:1000 (IF). Rabbit anti-aPKC (C-20 Santa Cruz), 1:500 (IF) 1:1000 (WB). Guinea pig anti-Par6, 1:250 (IF) 1:500 (WB) (A. Wodarz). Mouse anti-Notch-Extra (DSHB), 1:500 (IF). Mouse anti-Hindsight (DSHB), 1:100 (IF). Secondary antibodies labelled with Alexa dyes (Invitrogen), 1:1000 (IF). Secondary antibodies labelled with HRP (Santa Cruz), 1:3000 (WB), secondary antibodies labeled with alkaline phosphatase (Sigma) 1:2500.

**Western Blotting**

3$^{rd}$ instar larvae or wing discs were prepared for SDS page by washing in PBS, drying (larvae only) and then mashing in 50µl 2xSDS loading buffer (100mM Tris pH6.8, 4% SDS, 0.2% Bromophenol Blue, 20% glycerol, 2% beta-mercaptoethanol) using a 1.5ml Eppendorf tube and pestle. Samples were boiled, clarified by centrifugation and run on 8% SDS PAGE gels. Proteins were transferred to PVDF (Millipore), then probed using the antibodies described above.

**Immunofluorescence and Microscopy**
Wing discs were prepared for IF according to standard protocols [14]. Discs were fixed in 4% PFA for 20 min. Primary antibodies were incubated overnight at 4ºC. Secondary antibodies were incubated for 2 hr. Adult ovaries were dissected in ice cold PBS then fixed in 4% PFA for 20 min. Ovaries were then washed in PBT (PBS + 0.5% Triton-X 100), blocked in PBT + 5% BSA and incubated with primary antibodies overnight at 4ºC in block. Ovaries were washed with PBT, incubated in secondary antibodies (in block) for 2 hr at room temperature then washed with PBT and mounted in ProLong Gold (Invitrogen). Images were acquired using a Zeiss LSM 510 or a Zeiss LSM 710 NLO and processed using Fiji and Adobe Photoshop. All images shown are representative of the results obtained from several independent experiments (between 6 and 8 individual wing discs/ovary collections and stainings per genotype or chemical treatment).

**Leupeptin Experiment**
Ovaries were dissected in Schneider's medium containing 2.5% FCS and 5μg/ml Insulin and then incubated in the same supplemented with 100μg/ml leupeptin or the equivalent volume of water as a negative control rotating at room temperature for 3 hrs. To visualize lysosomal compartments, 1μl/ml Lysotracker was added to the rotating ovaries for the last 1 hr and the ovaries fixed as described previously. Images shown are representative of results obtained from 4 independent experiments.

**Immunostaining of HeLa Cells**
HeLa cells were seeded on collagen I coated coverslips and transfected with pcDNA-Flag-Crb2 (gift from Dr. Nishimura) [15] using JetPEI (Polyplus) according to the manufacturer's instructions. Cells were used for experiments 24 h after transfection, or, alternatively, cells were selected using 200μg/ml Zeocin (Melford) for stable expression of Flag-Crb2. Cells expressing Flag-Crb2 were labeled using anti Flag antibody clone M2 (Sigma) diluted 1:400 in culture medium and incubated at 37°C, 5% $CO_2$ for 90 min. Cells were chilled on ice, washed twice with ice-cold PBS followed by acid-stripping of surface bound antibody [16] for 4 min on ice and three washes with ice-cold PBS. Cells were fixed using 4% paraformaldehyde in PBS for 5 min on ice then 15 min at room temperature and processed as described previously [17]. Cells were stained using rabbit polyclonal Vps35 antibody (Millipore) or the previously described rabbit anti MPR antibody [18]. For studying Crb2 trafficking to lysosomes stably transfected, Flag-Crb2 expressing cells were incubated for 4 h at 37°C in normal growth medium containing protease inhibitor cocktail III (Fisher) as well as Flag antibody (1:400). Instead of formaldehyde fixation cells were fixed using Methanol for 5 min at -20°C followed by the standard procedure [17]. Imaging was performed using either a Leica AF6000 epifluorescence or a Leica SP5 confocal microscope with a 63x oil immersion objective. Images shown are representative of results obtained from at least three different experiments.

**RNAi Suppression of Vps35**
Vps35 was suppressed using Vps35-I: 5'-UUACAAGUCUCUCUGAUUA-3' or Vps35-II: 5'-GAACAUAUUGCUACCAGUA-3' (Dharmacon). Control siRNA targeting luciferase was obtained from Ambion. RNA duplexes were transfected using Interferin (Polyplus) at 10 nM final concentration according to the manufacturer's protocol. Cells were analyzed 3 days after transfection.

## Supplemental References


1. Carlton, J., Bujny, M., Peter, B.J., Oorschot, V.M., Rutherford, A., Mellor, H., Klumperman, J., McMahon, H.T., and Cullen, P.J. (2004). Sorting nexin-1 mediates tubular endosome-to-TGN transport through coincidence sensing of high- curvature membranes and 3-phosphoinositides. Curr Biol *14*, 1791-1800.
2. Wassmer, T., Attar, N., Harterink, M., van Weering, J.R., Traer, C.J., Oakley, J., Goud, B., Stephens, D.J., Verkade, P., Korswagen, H.C., et al. (2009). The retromer coat complex coordinates endosomal sorting and dynein-mediated transport, with carrier recognition by the trans-Golgi network. Dev Cell *17*, 110-122.
3. Seaman, M.N. (2004). Cargo-selective endosomal sorting for retrieval to the Golgi requires retromer. J Cell Biol *165*, 111-122.
4. Baust, T., Czupalla, C., Krause, E., Bourel-Bonnet, L., and Hoflack, B. (2006). Proteomic analysis of adaptor protein 1A coats selectively assembled on liposomes. Proc Natl Acad Sci U S A *103*, 3159-3164.
5. Crottet, P., Meyer, D.M., Rohrer, J., and Spiess, M. (2002). ARF1•GTP, Tyrosine-based Signals, and Phosphatidylinositol 4,5-Bisphosphate Constitute a Minimal Machinery to Recruit the AP-1 Clathrin Adaptor to Membranes. Mol. Biol. Cell *13*, 3672-3682.
6. Shevchenko, A., Tomas, H., Havlis, J., Olsen, J.V., and Mann, M. (2006). In-gel digestion for mass spectrometric characterization of proteins and proteomes. Nat Protoc *1*, 2856-2860.
7. Liu, H., Sadygov, R.G., and Yates, J.R., 3rd (2004). A model for random sampling and estimation of relative protein abundance in shotgun proteomics. Anal Chem *76*, 4193-4201.
8. Franch-Marro, X., Wendler, F., Guidato, S., Griffith, J., Baena-Lopez, A., Itasaki, N., Maurice, M.M., and Vincent, J.P. (2008). Wingless secretion requires endosome-to-Golgi retrieval of Wntless/Evi/Sprinter by the retromer complex. Nat Cell Biol *10*, 170-177.
9. Eugster, C., Pan·kov·, D., Mahmoud, A., and Eaton, S. (2007). Lipoprotein-Heparan Sulfate Interactions in the Hh Pathway. Developmental Cell *13*, 57-71.
10. Widmann, T.J., and Dahmann, C. (2009). Dpp signaling promotes the cuboidal-to-columnar shape transition of Drosophila wing disc epithelia by regulating Rho1. J Cell Sci *122*, 1362-1373.
11. Wodarz, A., Hinz, U., Engelbert, M., and Knust, E. (1995). Expression of crumbs confers apical character on plasma membrane domains of ectodermal epithelia of Drosophila. Cell *82*, 67-76.
12. Moline, M.M., Southern, C., and Bejsovec, A. (1999). Directionality of Wingless protein transport influences epidermal patterning in the Drosophila embryo. Development *126*, 4375-4384.
13. Tepass, U., Theres, C., and Knust, E. (1990). crumbs encodes an EGF-like protein expressed on apical membranes of Drosophila epithelial cells and required for organization of epithelia. Cell *61*, 787-799.
14. Sullivan, W., Ashburner, M., and Hawley, R.S. (2000). Drosophila protocols, (Cold Spring Harbor, N.Y.: Cold Spring Harbor Laboratory Press).
15. Mitsuishi, Y., Hasegawa, H., Matsuo, A., Araki, W., Suzuki, T., Tagami, S., Okochi, M., Takeda, M., Roepman, R., and Nishimura, M. (2010). Human CRB2 inhibits gamma-secretase cleavage of amyloid precursor protein by binding to the presenilin complex. J Biol Chem *285*, 14920-14931.
16. Carroll, R.C., Beattie, E.C., Xia, H., Loscher, C., Altschuler, Y., Nicoll, R.A., Malenka, R.C., and von Zastrow, M. (1999). Dynamin-dependent endocytosis of ionotropic glutamate receptors. Proceedings of the National Academy of Sciences of the United States of America *96*, 14112-14117.
17. Wassmer, T., Attar, N., Bujny, M.V., Oakley, J., Traer, C.J., and Cullen, P.J. (2007). A loss-of-function screen reveals SNX5 and SNX6 as potential components of the mammalian retromer. J Cell Sci *120*, 45-54.
18. Meresse, S., and Hoflack, B. (1993). Phosphorylation of the cation-independent mannose 6-phosphate receptor is closely associated with its exit from the trans-Golgi network. The Journal of Cell Biology *120*, 67-75.